Morindone From *Morinda Citrifolia* as a Potential Antiproliferative Agent Against Colorectal Cancer Cell Lines

Cheok Wui Chee
University of Malaya
Nor hisam Zamakshshari
University of Malaya
Vannajan Lee
University of Malaya
Iskandar Abdullah
University of Malaya
Rozana Othman
University of Malaya
Yean Kee Lee
University of Malaya
Najihah Mohd Hashim
University of Malaya
Nurshamimi Nor Rashid (nurshamimi@um.edu.my)
University of Malaya

Research Article

Keywords: Morindone, Morinda citrifolia, colorectal cancer, natural products, antiproliferative

Posted Date: July 21st, 2021

DOI: https://doi.org/10.21203/rs.3.rs-692423/v1

Abstract

There is an increasing demand in developing new, effective, and affordable anti-cancer against colon and rectal. In this study, our aim is to identify the potential anthraquinone compounds from the root bark of *Morinda citrifolia* to be tested *in vitro* against colorectal cancer cell lines. Eight potential anthraquinone compounds were successfully isolated, purified and tested for both *in-silico* and *in-vitro* analyses. Based on the *in-silico* prediction, two anthraquinones, morindone and rubiadin, exhibit a comparable binding affinity towards multitargets of β-catenin, MDM2-p53 and KRAS. Subsequently, we constructed a 2D interaction analysis based on the above results and it suggests that the predicted anthraquinones from *Morinda citrifolia* offer an attractive starting point for potential antiproliferative agents against colorectal cancer. *In vitro* analyses further indicated that morindone and damnacanthal have significant cytotoxicity effect and selectivity activity against colorectal cancer cell lines.

Introduction

Colorectal cancer (CRC) as a malignant cancer affecting both male and female, is ranked the third most common cancer worldwide and second most frequent cancer in Malaysia (GLOBOCAN 2020). Significant associations between dietary factors and CRC risk have been determined, in addition to smoking and alcohol intake (O'keefe, 2016). Regular consumption of fruits and vegetables was demonstrated effective in reducing CRC risk as polyphenolic compounds in plants contribute to decreasing cell adhesion process, migration, and tumour angiogenesis (Baena and Salinas, 2015). Standard chemotherapy regimens in treating CRC patients accommodates the use of cancer drug particularly 5-fluorouracil and doxorubicin hydrochloride that function by inhibiting DNA synthesis (Che and DeVita, 2015). Despite higher survival rate in patients, the adverse toxicity risk associated with these chemotherapy drugs need to be taken into account (Fotheringham et al, 2019). Therefore, the search for effective phytochemical compounds as antiproliferative agent continues.

Anthraquinone, an aromatic compound with a 9, 10-dioxoanthracene core can be found abundantly in several plants such as rhubarb root, aloe vera, morinda and senna leaf (Khan, 2019). It is reported to display pharmacological properties including anti-inflammatory, antioxidant, antimicrobial and anticancer (Duval et al., 2016). Zamakshshari et al. (2017) has reported that anthraquinone compounds obtained from *Morinda citrifolia* exhibited promising *in vitro* antitumor activity and selective against CRC cells. Following this, eight *Morinda citrifolia* isolated anthraquinone compounds were evaluated for cytotoxicity activity against CRC cell lines.

CRC is associated with a series of genetic alteration involving various pathway such as Wnt signalling pathway, Ras signaling pathway and p53 mediated apoptosis pathway. Being the crucial players of these pathway, β-catenin, p53 and KRAS genes are always found mutated in CRC, resulting in resistance to current therapies, conferring poor prognosis (Aran et al., 2016). Mologni et al. work in 2012 has reported promising combination therapeutic strategy in CRC by down regulating both β-catenin and KRAS simultaneously. Meanwhile, study by Hou et al. (2019) showed that the autoregulatory negative

feedback loop involving regulation of p53 by Murine Double Minute 2 (MDM2) could be a novel target therapy in cancer treatment as these two genes regulate each other mutually through an autoregulatory negative feedback loop. Plenty of evidence suggests the competent anticancer effect of anthraquinone against different genes and cancers, including our target genes: β-catenin (Liu et al., 2018; Pooja & Karunagaran, 2014; Zhang et al., 2015), MDM2-p53 (Balachandran et al., 2015; Draganov et al., 2019; Vanajothi & Srinivasan, 2016), and KRAS (Hiramatsu et al., 1993). With p53 and KRAS being the undruggable molecular targets, the discovery of new anticancer drugs for these genes by aiming the protein products (Lazo & Sharlow, 2016) and aided using computational techniques (Cui et al., 2020) have been reported. Thus, in this study, novel potential inhibitors based on anthraquinones from *Morinda citrifolia* were discovered through the deployment of ligand-based protein docking for β-catenin, MDM2-p53 and KRAS. Herewith, a correlation between structure conformation and cytotoxicity via both *in silico* and *in vitro* work was proposed.

Method And Material

2.1 Chemicals

All chemicals and solvents were purchased from Merck, Sigma-Aldrich and Fisher. MTT Cell Count Kit for cell cytotoxicity assay was purchased from Nacalai Tesque, Japan. 5-fluorouracil (5-FU) and doxorubicin hydrochloride were obtained from AoBo Bio-Pharmaceutical Technology, China and Santa Cruz, USA, respectively.

2.2 Plant Collection, extraction, and isolation of anthraquinone

The root bark of *Morinda citrifolia* was collected from Negeri Sembilan, Malaysia and authenticated by Professor Dr. Rusea Go from the Biology Department, Faculty of Science, Universiti Putra Malaysia. A voucher specimen (RG6085) was deposited in the Herbarium of Biology Department, Faculty of Science, Universiti Putra Malaysia. The study complies with national regulations and all necessary permits were obtained for the same.The collected plant sample was dried under open air and ground into fine powder. The powdered root bark of *Morinda citrifolia* was macerated three times in four different solvents: hexane, chloroform, ethyl acetate and methanol for 72 hours. The macerated sample was filtered and evaporated under reduced pressure to obtain dry extracts of methanol, ethyl acetate, chloroform, and hexane. Each extract was fractionated using vacuum column chromatography and resulted in 20-30 fractions. Then, each fraction underwent purification using two purification method which are gravity column chromatography and preparative thin layer chromatography. The isolation and purification of all extracts resulted in 8 anthraquinones as below:

Nordamnacanthal (1)

Yellow needle crystal; m.p: 219-222ºC (literature 218-220ºC, Prista *et al.,* 1965) IR v_{max} cm^{-1}: 2928, 1734, 1649, 1356, 1274; UV (EtOH) λmax 290 and 246nm; EI-MS m/z: 268, 240, 212, 184, 128, 69;^{1}H and ^{13}C-NMR spectra are in consistent with literature (Kamiya *et al.,* 2010).

Damnacanthal (2)

Yellow needle crystal; m.p: 208-210ºC (literature 211-212ºC, Horie *et al.,* 1956) IR v_{max} cm^{-1}: 2927, 1664, 1441, 1282 and 1116; UV (EtOH) λmax nm: 392 and 258; EI-MS m/z:282, 254, 225, 208, 139, 76, 63, 50; ^{1}H and ^{13}C- NMR spectra are in consistent with literature (Kamiya *et al.,* 2010).

1,3,5-trihydoxy-2-methoxy-6-methyl anthraquinone (3)

Yellow powder; m.p: 235-239ºC (literature 241ºC, Prista, *et al.,* 1965) IR v_{max} cm^{-1}: 3405, 2931, 1737, 1406, 1259 and 1161; UV (EtOH) λmax nm: 412 and 302; EI-MS m/z: 300,282,257,135,115,77,63,51. ^{1}H and ^{13}C-NMR spectra are in consistent with literature (Prista, *et al.,* 1965).

Morindone (4)

Orange-red needle crystal; m.p: 248-250ºC (literature 250-251ºC, Simonsen, 1918) IR v_{max} cm^{-1}: 2919, 2854, 1597, 1273 and 1072; UV (EtOH) λmax nm: 422 and 269; EI-MS m/z: 270,242, 139, 77, 69, 51.^{1}H and ^{13}C- NMR spectra are in consistent with literature (Kamiya *et al.,* 2010).

Sorendidiol (5)

Yellow needle crystal; m.p: 286-288ºC (literature 287-288ºC, Briggs *et al.,* 1952) IR v_{max} cm^{-1}:3295, 2930, 1740, 1561, 1440, 1294 and 1108; UV (EtOH) λmax nm: 412 and 320; EI-MS m/z: 254, 225, 197, 139, 115; ^{1}H and ^{13}C- NMR spectra are in consistent with literature (Kamiya *et al.,* 2010).

Rubiadin (6)

Yellow needle crystal; m.p: 288-290ºC (literature 290-291ºC, Chari *et al.,* 1966) IR v_{max} cm^{-1}: 3383, 2918, 1733, 1580, 1428, 1306 and 1106 UV (EtOH) λmax nm: 419, 324 and 225; EI-MS m/z: 254, 226, 197, 152, 115, 76; ^{1}H and ^{13}C-NMR spectra are in consistent with literature (Kamiya *et al.,* 2010).

Damnacanthol (7)

Yellow needle crystal; m.p: 156-158ºC (literature 157ºC, Horie *et al.,* 1965) IR v_{max} cm^{-1}: 3066, 2925, 1653, 1565, 1444, 1339 and 1258; UV (EtOH) λmax nm: 427, 282 and 215; EI-MS m/z:284, 269, 251, 237, 181, 152, 139, 76; ^{1}H and ^{13}C- NMR spectra are in consistent with literature (Horie *et al.,* 1965).

Lucidin-ω-methyether (8)

Orange-Yellow powder; m.p: 170-173ºC (literature 170ºC, Chang and Lee, 1984) IR v_{max} cm^{-1}: 3142, 2924, 1672, 1573, 1367, 1332 and 1273; UV(EtOH) λmax nm: 419, 325 and 226; EI-MS m/z: 284, 252, 196, 168; ^{1}H and ^{13}C- NMR spectra are in consistent with literature (Chang and Lee, 1984).

2.3 In silico investigation toward multi-protein targets in colorectal cancer

In order to elucidate the potential mechanism by which the active compounds induce the cytotoxic activity, molecular docking was performed to position the compounds into the active site of multiple targets; β-catenin (PDB ID: 1JDH), MDM2-p53 (PDB id: 4HG7) and KRAS (PDB ID: 5OCT), where the binding sites are as the following;

i. β-catenin binding sites: Site A of β-catenin contains the key important amino acid Lys312 (Binding center x, y, z: -6.30, 1.85, 50.08) while Site B contains amino acid Lys435 (Binding center x, y, z: -1.56, 10.65, 21.00) which is important in the interaction between the protein and the TCF4 protein (Graham *et al*., 2001)
ii. Crystal Structure of an MDM2/Nutlin-3a complex was used. MDM2-p53 binding site was selected from the ligand binding center at the position x, y, z: -24.55, 6.51, -13.83.
iii. Small molecule inhibitor of Ras-effector protein interactions in Xray structures was investigated and the ligand binding center at the position x, y, z: 64.00, 111.00, 1.81 was used.

All protein structures were prepared for docking using the protein preparation in Chimera software with default protocol for PDB2PQR and Dock Prep. Protonation state was assigned using PROPKA at pH 7.0 and gasteiger charges were assigned for protein (Peterson *et al*., 2004). Eight anthraquinone structures were downloaded from PubChem database except compounds **3, 5, 8** were modified from damnacanthol. All structures were optimized using PM6 level using Gaussian software package. Molecular docking was performed with local search algorithm using Autodock Vina in PyRx virtual screening software (http://pyrx.scripps.edu/). The prediction incorporated the target conformation as a rigid unit meanwhile allowing the ligands to be flexible and adaptable to the target. The amino acid binding sites were selected at the binding sites from the information above. Grid box was set at 20 x 20 x 20 $Å^3$ with the default grid spacing of 0.375. The 3D structures were visualized by YASARA (http://www.yasara.org/index.html) and 2D interaction was analyzed by BIOVIA Discovery Studio software (Dassault Systèmes BIOVIA, Discovery Studio Modeling Environment, Release 2018, San Diego: Dassault Systèmes, 2016). Different conformations for each ligand and the lowest binding affinity conformations were predicted.

2.4 Cell Lines

Colorectal cancer cell lines: HT29, HCT116 and LS174T as well as normal colon cells, CCD841 CoN were obtained from American Type Cell Culture (Manassas, VA). All cell lines were cultured in an incubator under the condition of 37°C temperature, humidified 5% CO_2 air atmosphere. Cells were maintained in Dulbecco's Modified Eagle Medium (DMEM) supplemented with 10% Fetal Bovine Serum (FBS), HEPES and 1% Penicillin/Streptomycin.

2.5 Cell Cytotoxicity Assay

Cells were seeded at 3 x 10^4 cells/well in 96 well plates and allowed for 24 hours incubation. Cells were then treated with anthraquinone compounds at series of concentrations (50μM, 25μM, 12.5μM, 6.25μM, 3.12μM, 1.56μM, 0.78μM, 0.39μM) for 72 hours. 5-FU and doxorubicin hydrochloride were used as positive controls in the treatment. Cell cytotoxicity was measured using the MTT Cell Count kit (Nacalai Tesque, Japan) according to the manufacturer's protocol.

2.6 Selectivity Index

Selective index (SI) value was calculated based on how much each anthraquinone compound is selective towards CRC cells in comparison with normal cell. SI value was calculated using the formula below:

$$\text{Selectivity Index} = \frac{\text{IC}_{50} \text{ in normal cells}}{\text{IC}_{50} \text{ in cancer cells}}$$

2.7 Statistical Analysis

Statistical analysis was performed using GraphPad PRISM. All data were presented as mean. P value <0.05 is considered significant. Dunnett's Post Hoc Test after one-way analysis of variance (ANOVA) was carried out to compare each treatment group against control group.

Results And Discussion

Isolation and purification of *Morinda citrifolia*

The root of *Morinda citrifolia* (3.0 kg) was extracted using macerated method in methanol (60 g), ethyl acetate (54 g), chloroform (38 g) and hexane (31 g). These crude extracts were then subjected under column and preparative thin layer chromatography which resulted in eight types of anthraquinone. Four out of eight anthraquinones were successfully isolated from the hexane extract namely nordamnacanthal (1) (27mg), damnacanthal (2) (3mg), 1,3,5-dihydoxy-2-methoxy-6-methyl anthraquinone (3) (3mg), and morindone (4) (15mg). Meanwhile, other anthraquinones were successfully isolated from the semi polar solvent namely sorendidiol (5) (21mg), rubiadin (6) (9.8mg), damnacanthol (7) (69.9mg) and lucidin-ω-methyether (8) (74.7mg). The ^{1}H and ^{13}C nuclear magnetic resonance (NMR) spectroscopic data (Supplementary Materials) for compounds 1, 2, 4, 5, 6 were in consistence with literature Kamiya et al. (2010). While compounds 3, 7 and 8 were in consistence with literature Prista, et al. (1965), Horie et al.

(1965) and Chang and Lee (1984), respectively. The chemical structures of all anthraquinones were illustrated in Figure 1.

Docking of anthraquinones and binding interaction towards multitargets in colorectal cancer

Molecular docking was performed to determine the interaction between 8 isolated anthraquinones and the targeted protein receptors in cancer cell to explore the relationship between chemical structure and bioactivity. Results from molecular docking was validated using the bound inhibitors and redocked to its original position in the X-ray crystal structure. This binding model derived from a molecular docking was used to understand the anticancer mechanism at molecular level towards three targets, β-catenin, MDM2-p53, and KRAS. From our previous study (Fatima et al., 2018), the Wnt–β-catenin pathway appears to be deregulated in most cancer cells including breast and CRC where the inhibition mechanism is involved with the binding of free β-catenin in the cytoplasm and the β-catenin–transcription factor 4 complex in the nucleus at the β-catenin binding pocket with amino acid residues, Lys345, Trp383, Arg386 and Asn415. Similarly, the inhibitions of MDM2 protein and KRAS were controlled by the binding of inhibitor toward the binding pocket. The p53 binding pocket on MDM2 protein was selected where it controls the activity of p53 protein through working as ubiquitin E3 ligase promoting p53 degradation through the proteasome degradation pathway (Atatreh et al., 2018) whereas the binding of ligand on a defined KRAS active site will regulate the cell growth, differentiation, and apoptosis through several signalling pathways (Hashemi et al., 2020).

Among the eight isolated anthraquinones tested, morindone, showed the highest inhibition against multiple targets in CRC which include β-catenin, MDM2-p53, and KRAS as reported in Table 1. Another interesting compound having comparable binding affinity with morindone is rubiadin. Both docked complexes are selected for a binding mode analysis. The three-dimensional structure of morindone (cyan) and rubiadin (yellow) against β-catenin with the TCF cofactor shown in red, MDM2-p53, and KRAS where molecular surface regarding residues type in 3 Å binding with compounds were illustrated in Figure 2. Amino acid residue types are coloured by YASARA colouring scheme: nonpolar, grey; amidic, green; basic, blue; acidic, red; hydroxylic, cyan. A 2D binding mode inspection using Biovia Discovery Studio (Figure 3) revealed the important binding interactions of morindone and rubiadin with residues at the binding site of protein receptors.

In the case of binding with β-catenin, all anthraquinones preferred to bind at hydrophobic pocket site A where the important amino acids in chain A are Gln,309, Lys312, Val349, Cys350, Ser351, Ser352 and residues in TCF cofactors in chain B are Glu29, Lys30. Lys312 was identified as the key amino acids in this binding pocket in several reports (Graham et al., 2001; Yu et al., 2013). Rubiadin bound different pattern in the same pocket with slightly more favourable interaction of -6.6 kcal/mol compared to -5.9 kcal/mol for morindone. Rubiadin exhibits better binding due to hydrogen bond interaction of carbonyl oxygen with Lys312 where oxygen atom of the chelated hydroxyl in morindone was found to have hydrogen bonding with Ser351, not with Lys312. Another interaction type, π-sulfur interaction with Cys350 was also shown in Table 2.

Targeting MDM2-p53 interaction received great attention. Overexpression of MDM2 and subsequent deactivation of p53 protein resulted in failure of apoptosis and cancer cell survival ((Klein and Vassilev 2004; Shangary and Wang, 2009; Selivanova, 2010; Stegh, 2012; Essmann and Schulze-Osthoff, 2012). In previous study, 14 amino acids form a deep hydrophobic cavity on the MDM2 protein structure that can be occupied by small molecule inhibitors; Leu54, Leu57, Ile61, Met62, Tyr67, Gln72, Val75, Phe86, Phe91, Val93, His96, Ile99, Tyr100, and Ile101 (Atatreh et al., 2018). From our *in-silico* investigation, morindone and rubiadin have the same binding affinity of -7.1 kcal/mol. The binding pocket includes nonpolar residues; Ile19, Gln24, Lys51, His96, Tyr100 and polar residues; Leu54, Val93, and Ile99 where the vdW and π-Alkyl interactions were dominated, respectively. Another type of interaction, π-π stacking was observed in rubiadin and His96.

KRAS are the most frequently mutated oncogenes in human cancer among the three human Ras genes (KRAS, NRAS and HRAS) appearing in 45% of CRC which makes Ras one of the most crucial targets in oncology for drug development (Cox et al., 2014). Morindone exhibits the best scores among the tested anthraquinones with a binding affinity of -8.5 kcal/mol toward KRAS where its interactions with β-catenin and MDM2-p53 were -5.9 and -7.1 kcal/mol, respectively. Two oxygen atoms of the chelated hydroxyl formed H-bond interactions with Lys117. π-Alkyl interaction with Ala18, Tyr32, Ala146 and π-π stacked interaction with Phe28 of the planar benzyl ring in morindone have been observed. Besides, the nonpolar interaction in the hydrophobic pockets of Lys117, Asn116, Leu120, Ser145, Lys147, Thr148 was observed. On the other hand, different binding mode of interaction of rubiadin were due to two hydrogen bonding of carbonyl oxygen and oxygen atoms of the chelated hydroxyl with Ala18, Asn116; π-Anion interaction with Lys117; π-Alkyl interaction with Tyr32, Leu120; π-π stacked interaction with Phe28; and hydrophobic interaction with Gly15, Lys16, Ser17, Ala18, Val29, Asp30, Glu31, Asp33, Ser145, Asn116. A similar trend was demonstrated by rubiadin that bound better with KRAS, MDM2, and β-catenin at a binding affinity of -7.7, -7.1, and -6.6, respectively.

The binding pattern in this study was referred to the virtual screening from our previous study. Unfortunately, an *in vitro* experiment to validate the binding mode for these three protein targets was not performed due to fund limitation.

Cytotoxic Activity Evaluation

All compounds were evaluated with cytotoxicity test using MTT assay on normal colon, CCD841 CoN cells and 3 CRC cell lines, HCT116 cells, LS174T cells and HT29 cells. The IC_{50} values are presented in Table 3. Selectivity index (SI) which indicates the cytotoxicity selectivity was also calculated using IC_{50} value of normal colon (CCD841 CoN cells) against IC_{50} value of colorectal cancer cell lines and presented in Table 4. The bigger the SI value, the more selective it is. An SI value lower than 2 indicate general toxicity of the pure compound (Badisa et al., 2009).

Generally, damnacanthal, 1,3,5-trihydoxy-2-methoxy-6-methyl anthraquinone, morindone, damnacanthol and lucidin-ω-methyether has IC_{50} value lower than 25μM on HCT116 cells. Damnacanthal, morindone

and sorendidiol has slightly higher IC_{50} value ranged between 19μM and 30μM on HT29 cells (Figure 4). Only morindone has cytotoxic effect on LS174T cells at IC_{50} value of 20.45μM (Figure 5) while nordamnacanthal and rubiadin has IC_{50} value greater than 50μM for all cell lines. Overall, all anthraquinone compounds have no significant cytotoxicity effect on the normal colon cells, CCD841 CoN cells (Figure 6).

An IC_{50} value as low as 0.74μM was exhibited by damnacanthal towards HCT116 cells, which is comparable with IC_{50} value of 5-FU and doxorubicin. Data shows that damnacanthal has relatively high SI value, 951.60 towards HCT116 cells and 24.85 towards HT29 cells. Good anticancer and antitumor activities by damnacanthal towards MCF-7 cells (breast cancer), HCT116 cells (colorectal cancer) and HepG2 cells (hepatocellular carcinoma) were also reported by Abdul Aziz et al. (2014), Nualsanit et al. (2012) and García-Vilas et al. (2015). A dose-dependent manner of antiproliferative activity of damnacanthal treated cancer cells was shown by García-Vilas et al. (2015) which corresponds with this study. The strong cytotoxicity activity of damnacanthal is highly linked to the presence of a hydroxyl at C-1 and hydroxylated at C-3 (Ali et al., 2000). Despite of a moderate binding affinity on three protein targets was exhibited by damnacanthal, this compound has displayed significant cytotoxic effect and selectivity index towards HCT116 cells, which are comparable to the standard drugs, 5-FU and doxorubicin hydrochloride. Therefore, damnacanthal could be a promising candidate in targeting KRAS mutation in CRC as HCT116 cells carry KRAS gene mutation.

Meanwhile, morindone also has high cytotoxicity effect towards all three CRC cell lines. The IC_{50} value of morindone for HCT116 cells is 10.70μM, 20.45μM for LS174T cells and 19.20μM for HT29 cells. Morindone is selective towards all three CRC cell lines with SI value of 76.25 for HCT116 cells, 39.89 for LS174T cells and 42.49 for HT29 cells. This is in concordance with the molecular docking results obtained. Among 8 anthraquinones, morindone has the strongest binding affinity towards MDM2-p53 and KRAS. This indicates that morindone is favourable for targeting the p53 and KRAS mutation in CRC. The high degree of cytotoxicity effect performed by morindone could be due to the formyl group appear at 1,2-dihydroxyl group (Ali et al., 2000). The inhibitory effect of morindone on HCT116 cell proliferation was also reported in work by Kamiya et al. (2010). Other than that, morindone also demonstrated strong antimicrobial activity against *C. lipolytica* (Ali et al., 2010) and oxacillin-resistant *Staphylococcus aureus* (Borotto et al., 2010)

Conclusion

In conclusion, among the 8 anthraquinones, morindone showed high cytotoxicity effect and great selectivity index towards colorectal cancer cell lines as well as strong binding affinities in *in-vitro* and *in-silico* investigation towards multiple protein targets of β-catenin, MDM2-p53, and KRAS in comparison to other anthraquinones. Molecular docking result showed that all the active compounds can bind well into each targeted protein receptor by binding to important residues in the protein, explaining their inhibitory activities. Interesting binding activity of selected anthraquinones were contributed by the presence of

several hydrogen bonds from carbonyl oxygen, oxygens at chelate hydroxyl, Van der Waals forces, and π-interactions of the planar benzyl ring. Further *in vivo* assays towards morindone are needed for the development of potential lead compound against colorectal cancer cells.

Declarations

Acknowledgment

The authors would like to acknowledge financial support from Universiti Malaya under IIRG-003A-2019, IIRG-003B-2019 and IIRG-003C-2019 research grants and research facilities.

References

1. Abdul Aziz, M. Y., Omar, A. R., Subramani, T., Yeap, S. K., Ho, W. Y., Ismail, N. H., ... & Alitheen, N. B. (2014). Damnacanthal is a potent inducer of apoptosis with anticancer activity by stimulating p53 and p21 genes in MCF-7 breast cancer cells. *Oncology letters*, *7*(5), 1479-1484.
2. Ali, A. M., Ismail, N. H., Mackeen, M. M., Yazan, L. S., Mohamed, S. M., Ho, A. S. H., & Lajis, N. H. (2000). Antiviral, cytotoxic and antimicrobial activities of anthraquinones isolated from the roots of Morinda elliptica. *Pharmaceutical Biology*, *38*(4), 298-301.
3. Atatreh, N., Ghattas, M. A., Bardaweel, S. K., Al Rawashdeh, S., & Al Sorkhy, M. (2018). Identification of new inhibitors of Mdm2–p53 interaction via pharmacophore and structure-based virtual screening. Drug design, development and therapy, 12, 3741.
4. Aran, V., Victorino, A. P., Thuler, L. C., & Ferreira, C. G. (2016). Colorectal Cancer: Epidemiology, Disease Mechanisms and Interventions to Reduce Onset and Mortality. *Clinical colorectal cancer*, *15*(3), 195–203.
5. Badisa, R. B., Darling-Reed, S. F., Joseph, P., Cooperwood, J. S., Latinwo, L. M., & Goodman, C. B. (2009). Selective cytotoxic activities of two novel synthetic drugs on human breast carcinoma MCF-7 cells. *Anticancer research*, *29*(8), 2993-2996.
6. Baena, R., & Salinas, P. (2015). Diet and colorectal cancer. *Maturitas*, *80*(3), 258-264.
7. Balachandran, C., Duraipandiyan, V., Al-Dhabi, N. A., Stalin, A., Balakrishna, K., Ignacimuthu, S., & Tilton, F. (2015). Isolation and characterization of Anthraquinone from Streptomyces sp. ERINLG-26 with anticancer activity against adenocarcinoma cell line COLO320. *Applied biochemistry and microbiology*, *51*(5), 522-529.
8. BIOVIA Discovery Studio software (Dassault Systèmes BIOVIA, Discovery Studio Modeling Environment, Release 2018, San Diego: Dassault Systèmes, 2016).
9. Borroto, J., Salazar, R., Pérez, A., Quiros, Y., Hernandez, M., Waksman, N., & Trujillo, R. (2010). Antimicrobial activity of the dichloromethane extract from in vitro cultured roots of Morinda royoc and its main constituents. *Natural product communications*, *5*(5), 1934578X1000500526

10. Briggs, L. H., Nicholls, G. A., and Peterson, R. M. L., (1952). Chemistry of the Coprosma genus. VI Minor antraquinone coloring matters from *Cosprosma australlis. Journal of Chemistry Society* 3:1718-1722.
11. Chari, V.M., Neelakantan, S. and Seshadri, T.R., (1966). Rubidin. *India Journal of chemistry* 4: 330-331.
12. Chang, P., and Lee, K. H., (1984). Cytotoxic antileukimic antraquinones from *Morinda parvifolia*. *Phytochemistry*, 23(8):1733-1736.
13. Chu, E., & DeVita, V. T. (2015). Physicians' Cancer Chemotherapy Drug Manual 2015. Burlington, MA: Jones & Bartlett Learning. pp. 164-168, 203-206.
14. Cui, W., Aouidate, A., Wang, S., Yu, Q., Li, Y., & Yuan, S. (2020). Discovering anti-cancer drugs via computational methods. *Frontiers in Pharmacology*, *11*: 733-747.
15. Cox, A. D., Fesik, S. W., Kimmelman, A. C., Luo, J., & Der, C. J. (2014). Drugging the undruggable RAS: mission possible?. Nature reviews Drug discovery, 13(11), 828-851.
16. Draganov, A. B., Yang, X., Anifowose, A., De La Cruz, L. K. C., Dai, C., Ni, N., ... & Wang, B. (2019). Upregulation of p53 through induction of MDM2 degradation: Anthraquinone analogs. *Bioorganic & medicinal chemistry*, *27*(17), 3860-3865.
17. Essmann, F., & Schulze-Osthoff, K. (2012). Translational approaches targeting the p53 pathway for anti-cancer therapy. British journal of pharmacology, 165(2), 328-344.
18. Fatima, A., Abdul, A. B. H., Abdullah, R., Karjiban, R. A., & Lee, V. S. (2018). Docking studies reveal zerumbone targets β-catenin of the Wnt–β-catenin pathway in breast cancer. *Journal of the Serbian Chemical Society*, 83(5), 575-591.
19. Filho, C., Meyre, V., Silva, C., & Niero, R. (2009). Chemical and pharmacological aspects of the genus Calophyllum. *Chemistry & Biodiversity* 6(3):313-327.
20. Fotheringham, S., Mozolowski, G. A., Murray, E., & Kerr, D. J. (2019). Challenges and solutions in patient treatment strategies for stage II colon cancer. *Gastroenterology report*, *7*(3), 151–161. https://doi.org/10.1093/gastro/goz006
21. García-Vilas, J. A., Quesada, A. R., & Medina, M. A. (2015). Damnacanthal, a noni anthraquinone, inhibits c-Met and is a potent antitumor compound against Hep G2 human hepatocellular carcinoma cells. *Scientific reports*, *5*, 8021.
22. GLOBOCAN. (2020). Colorectal cancer. Retrieved from https://gco.iarc.fr/today/fact-sheets-cancers
23. Graham, T.A., Ferkey, D.M., Mao, F., Kimelman, D., & Xu, W. (2001) Tcf4 can specifically recognize beta-catenin using alternative conformations. *Nat Struct Biol* 8: 1048-1052.
24. Hashemi, S., Sharifi, A., Zareei, S., Mohamedi, G., Biglar, M., & Amanlou, M. (2020). Discovery of direct inhibitor of KRAS oncogenic protein by natural products: a combination of pharmacophore search, molecular docking, and molecular dynamic studies. *Research in Pharmaceutical Sciences*, 15(3), 226.

25. Hiramatsu, T., Imoto, M., Koyano, T., & Umezawa, K. (1993). Induction of normal phenotypes in ras-transformed cells by damnacanthal from Morinda citrifolia. *Cancer letters*, *73*(2-3), 161–166.
26. Horie, Y. (1956). Synthesis of damnacanthol and damnacanthal. *Yakugaku Zasshi* 76:1448-1449.
27. Hou, H., Sun, D. & Zhang, X. (2019). The role of *MDM2* amplification and overexpression in therapeutic resistance of malignant tumors. *Cancer Cell Int*ernational (19), 216.
28. Kamiya, K., Hamabe, W., Tokuyama, S., Hirano, K., Satake, T., Kumamoto-Yonezawa, Y., Yoshida H., and Mizushina, Y., (2010). Inhibitory effect of anthraquinones isolated from the Noni (Morinda citrifolia) root on animal A-, B- and Y-families of DNA polymerases and human cancer cell proliferation. *Food Chemistry* 118:725–730.
29. Khan, N . T. (2019) Anthraquinones - A Naturopathic Compound. *Journal of New Developments in Chemistry* , *2*(2):25-28.
30. Klein, C., & Vassilev, L. T. (2004). Targeting the p53–MDM2 interaction to treat cancer. British journal of cancer, 91(8), 1415-1419.
31. Lazo, J. S., & Sharlow, E. R. (2016). Drugging undruggable molecular cancer targets. Annual review of pharmacology and toxicology, 56, 23-40.
32. Liu, S., Wang, J., Shao, T., Song, P., Kong, Q., Hua, H., ... & Jiang, Y. (2018). The natural agent rhein induces β-catenin degradation and tumour growth arrest. *Journal of cellular and molecular medicine*, *22*(1), 589-599.
33. Mologni, L., Brussolo, S., Ceccon, M., & Gambacorti-Passerini, C. (2012). Synergistic effects of combined Wnt/KRAS inhibition in colorectal cancer cells. *PloS one*, *7*(12), e51449.
34. Nualsanit, T., Rojanapanthu, P., Gritsanapan, W., Lee, S. H., Lawson, D., & Baek, S. J. (2012). Damnacanthal, a noni component, exhibits antitumorigenic activity in human colorectal cancer cells. *The Journal of nutritional biochemistry*, *23*(8), 915-923.
35. O'keefe, S. J. (2016). Diet, microorganisms and their metabolites, and colon cancer. *Nature reviews Gastroenterology & hepatology*, *13*(12), 691.
36. Pettersen, E. F., Goddard, T. D., Huang, C. C., Couch, G. S., Greenblatt, D. M., Meng, E. C., & Ferrin, T. E. (2004). UCSF Chimera—a visualization system for exploratory research and analysis. Journal of computational chemistry, 25(13), 1605-1612.
37. Pooja, T., & Karunagaran, D. (2014). Emodin suppresses Wnt signaling in human colorectal cancer cells SW480 and SW620. *European journal of pharmacology*, *742*, 55-64.
38. Prista, L. N., Roque, A. S., Ferreira, M.A. and Alves, A. C., (1965). Chemical study of *Morinda geminates*. I. Isolation of morindone, damnacanthal, nor-damnacanthal and rubiadin-1-methyl ether. *Garcia de Orta* 13: 19-38.
39. Simonsen, J.L., (1918). LXVI- Morindone. *J. Chem. Soc trans* 113:766-774.
40. Samoylenko, V., Zhao, J., Dunbar, D. C., Khan, I. A., Rushing, J. W., and Muhammad, I., (2006). New Constituents from Noni (*Morinda citrifolia*) Fruit Juice, *J. Agric. Food Chem.* 54:6398-6402.

41. Selivanova, G. (2010, February). Therapeutic targeting of p53 by small molecules. In Seminars in cancer biology (Vol. 20, No. 1, pp. 46-56). Academic Press.
42. Shangary, S., & Wang, S. (2009). Small-molecule inhibitors of the MDM2-p53 protein-protein interaction to reactivate p53 function: a novel approach for cancer therapy. Annual review of pharmacology and toxicology, 49, 223-241.
43. Selvan, V., (2007). Trees and shrubs of the Maldives, thammada press Co., Ltd., Bangkok,2007, ©FAO regional office for Asia and the pacific.
44. Stegh, A. H. (2012). Targeting the p53 signaling pathway in cancer therapy–the promises, challenges and perils. Expert opinion on therapeutic targets, 16(1), 67-83.
45. Vanajothi, R., & Srinivasan, P. (2016). An anthraquinone derivative from Luffa acutangula induces apoptosis in human lung cancer cell line NCI-H460 through p53-dependent pathway. *Journal of Receptors and Signal Transduction*, *36*(3), 292-302.
46. Yu, B., Huang, Z., Zhang, M., Dillard, D. R., & Ji, H. (2013). Rational Design of Small-Catenin/T-by Bioisostere Replacement, ACS Chem. Biol, 8, 18-23.
47. Zamakshshari N.H., Lian Ee G.C., Mah S.H., Ibrahim Z, Teh S.S., et al. (2017) Cytotoxic Activities of Anthraquinones from *Morinda citrifolia* towards SNU-1 and LS-174T and K562 Cell Lines. *Archives of Natural and Medicinal Chemistry 2017*, (ANMC-110).
48. Zhang, F. Y., Hu, Y., Que, Z. Y., Wang, P., Liu, Y. H., Wang, Z. H., & Xue, Y. X. (2015). Shikonin inhibits the migration and invasion of human glioblastoma cells by targeting phosphorylated β-catenin and phosphorylated PI3K/Akt: A potential mechanism for the anti-glioma efficacy of a traditional Chinese herbal medicine. *International journal of molecular sciences*, *16*(10), 23823-23848.

Tables

Table 1. Binding affinity of anthraquinones towards three protein targets in colorectal cancer. The best scores were highlighted in bold letter.

Compounds	Binding Affinity (kcal/mol)			
	β-catenin		MDM2-p53	KRAS
	Site A	Site B		
Nordamnacanthal (1)	**-6.6**	-4.8	-6.9	-7.6
Damnacanthal (2)	-5.7	-5.1	-6.6	-7.6
1,3,5-trihydoxy-2-methoxy-6-methyl anthraquinone (3)	-5.6	**-5.2**	-6.8	-7.2
Morindone (4)	-5.9	-4.9	**-7.1**	**-8.5**
Sorendidiol (5)	-5.8	-4.7	**-7.1**	-8.2
Rubiadin (6)	**-6.6**	-4.7	**-7.1**	-7.7
Damnacanthol (7)	-5.4	-5.0	-6.7	-7.6
Lucidin-ω-methyether (8)	-6.3	-4.6	-7.0	-7.4

Table 2. Two-dimensional diagram of residues binding interaction of morindone and rubiadin with β-catenin (Site A), MDM2-p53, and KRAS. Each residue is colored by the type of interaction; van der Waals (light green), hydrogen bond (green), and polar (magenta and orange).

Compounds	Binding Affinity (kcal/mol)		
	β-catenin (Site A)	MDM2-p53	KRAS
Morindone	-5.9	-7.1	-8.5
Rubiadin	-6.6	-7.1	-7.7

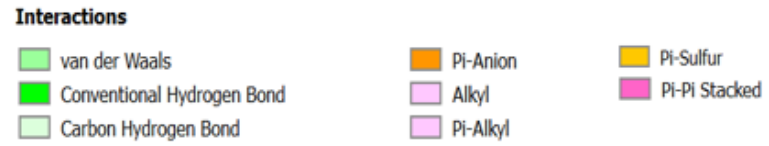

Table 3. The IC_{50} value of anthraquinone compounds 1-8, 5-Fluorouracil, and doxorubicin hydrochloride on colorectal cancer cell lines and normal colon cells after 72 hours treatment.

Anthraquinone Compound	IC_{50} (μM)			
	HCT116	LS174T	HT29	CCD841 CoN
Nordamnacanthal (1)	>50	>50	>50	>50
Damnacanthal (2)	**0.74 ± 0.06**	>50	**28.17 ± 0.08**	>50
1,3,5-trihydoxy-2-methoxy-6-methyl anthraquinone (3)	24.57 ± 0.07	>50	>50	>50
Morindone (4)	**10.70 ± 0.04**	**20.45 ± 0.03**	**19.20 ± 0.05**	>50
Sorendidiol (5)	>50	>50	27.17 ± 0.07	>50
Rubiadin (6)	>50	>50	>50	>50
Damnacanthol (7)	18.47 ± 0.02	>50	>50	>50
Lucidin-ω-methyether (8)	14.88 ± 0.01	>50	>50	>50
5-Fluorouracil	5.0 ± 0.04	4.16 ± 0.02	0.2 ± 0.05	-
Doxorubicin hydrochloride	0.17 ± 0.04	2.27 ± 0.04	0.3 ± 0.06	-

Table 4. Selectivity index of normal colon cells against colorectal cancer cells.

Compound	HCT116	LS174T	HT29
Nordamnacanthal (1)	0.97	4.79	0.42
Damnacanthal (2)	**951.60**	0.28	**24.85**
1,3,5-trihydoxy-2-methoxy-6-methyl anthraquinone (3)	4.55	0.97	0.03
Morindone (4)	**76.25**	**39.89**	**42.49**
Sorendidiol (5)	7.10	<0	**29.19**
Rubiadin (6)	<0	<0	<0
Damnacanthol (7)	<0	0.59	1.46
Lucidin-ω-methyether (8)	<0	<0	<0

Figures

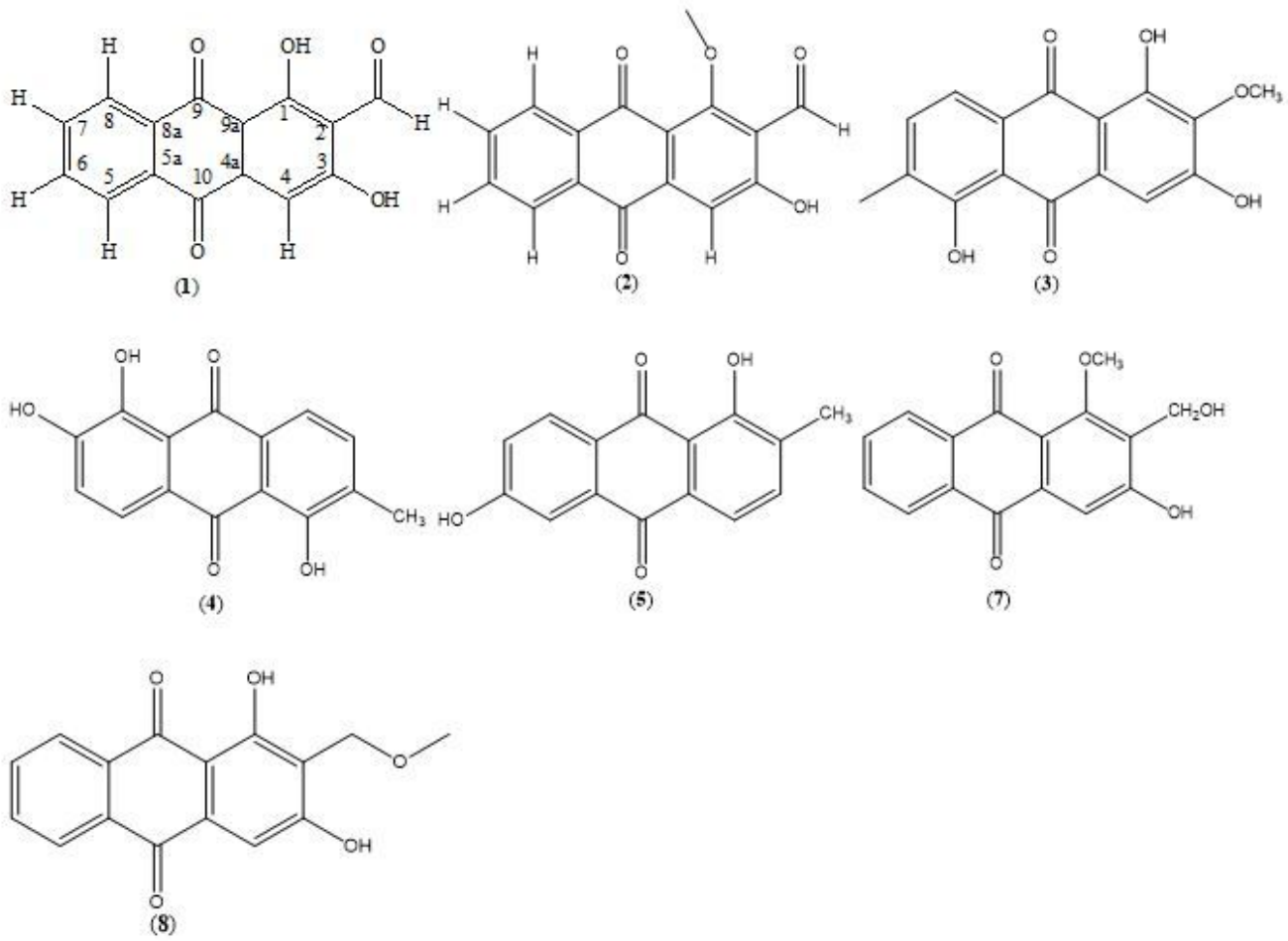

Figure 1

Chemical structure of nordamnacanthal (1), damnacanthal (2), 1,3,5-dihydoxy-2-methoxy-6-methyl anthraquinone (3), morindone (4), sorendidiol (5), rubiadin (6), damnacanthol (7) and lucidin-ω-methyether (8).

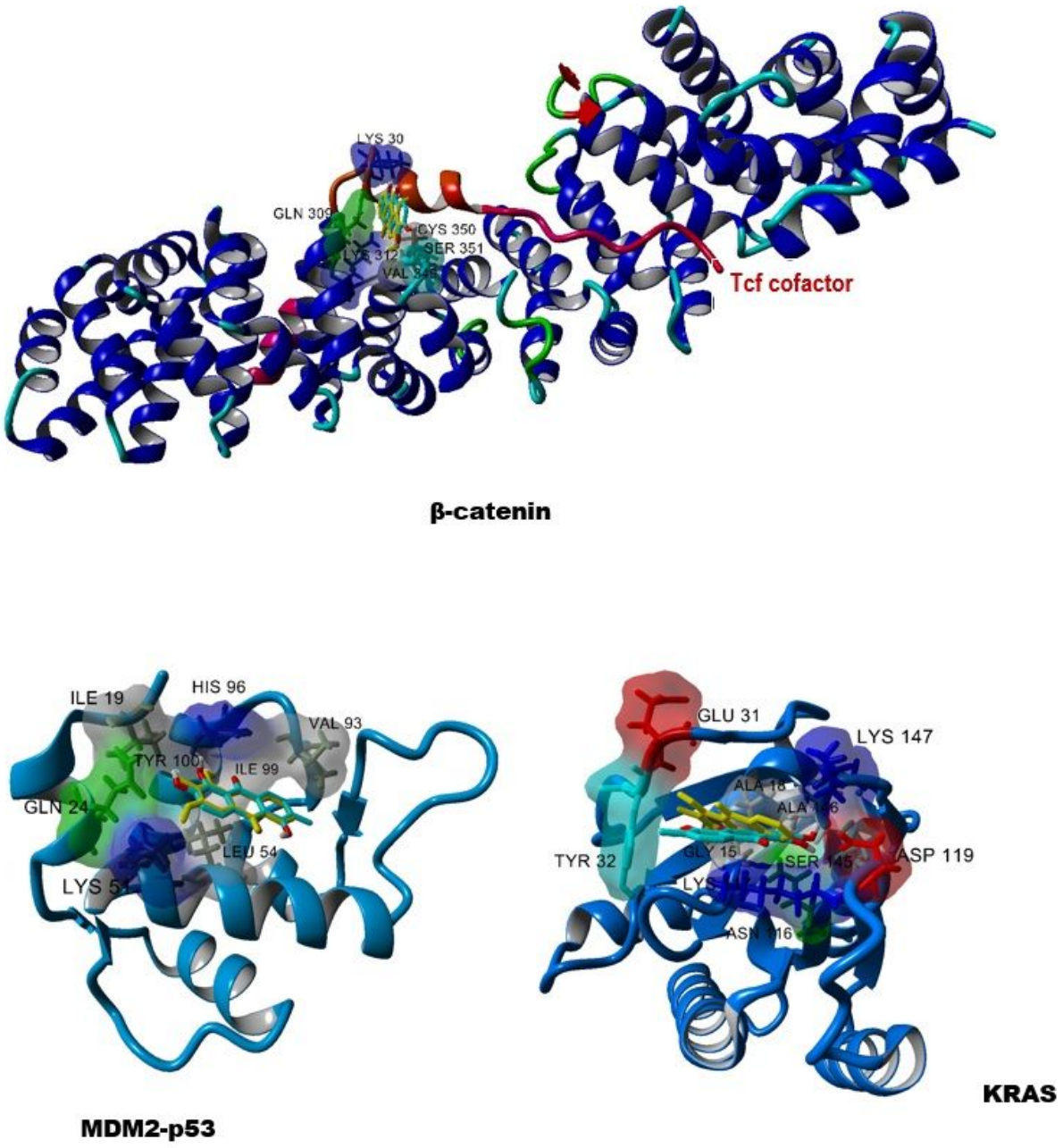

Figure 2

Docking complex of morindone (cyan) and rubiadin (yellow) against β-catenin where the TCF cofactor are shown in red, MDM2-p53, and KRAS. Molecular surface regarding residues type at the binding residues within 3 Å from compounds were illustrated. Amino acid residue types are colored by YASARA coloring scheme: nonpolar, grey; amidic, green; basic, blue; acidic, red; hydroxylic, cyan

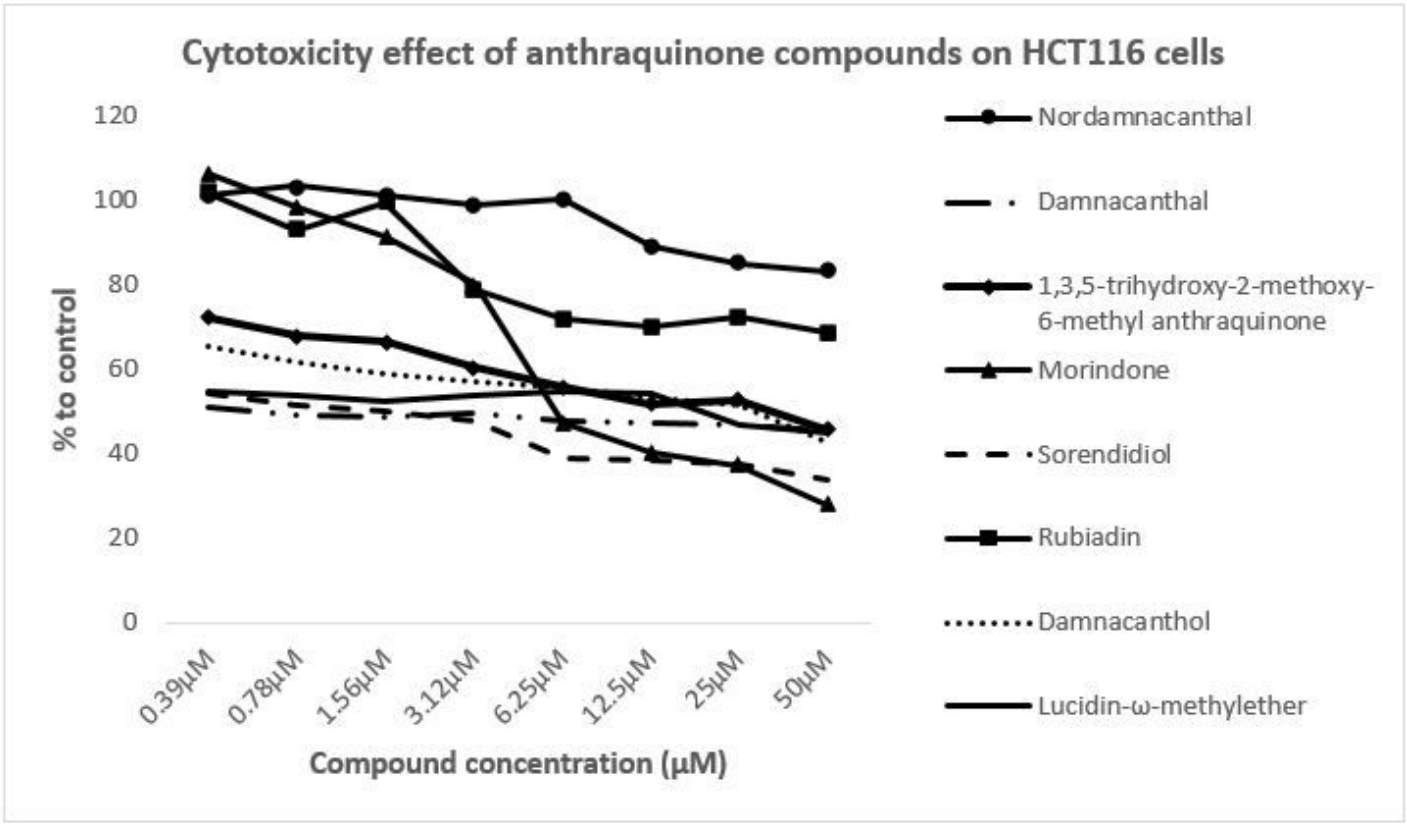

Figure 3

Cytotoxicity effect of anthraquinone compounds 1-8 on HCT116 cells after 72 hours treatment.

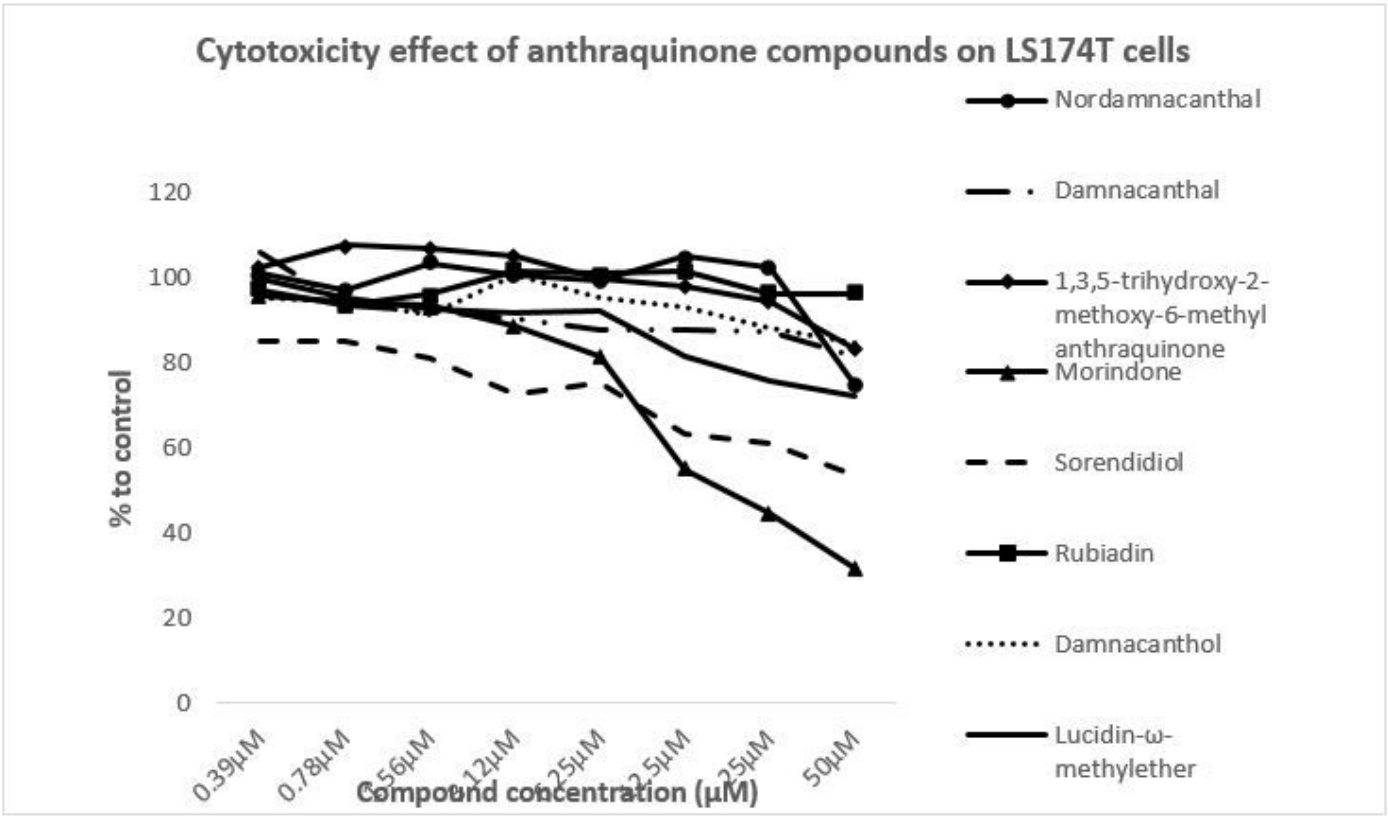

Figure 4

Cytotoxicity effect of anthraquinone compounds 1-8 on LS174T cells after 72 hours treatment.

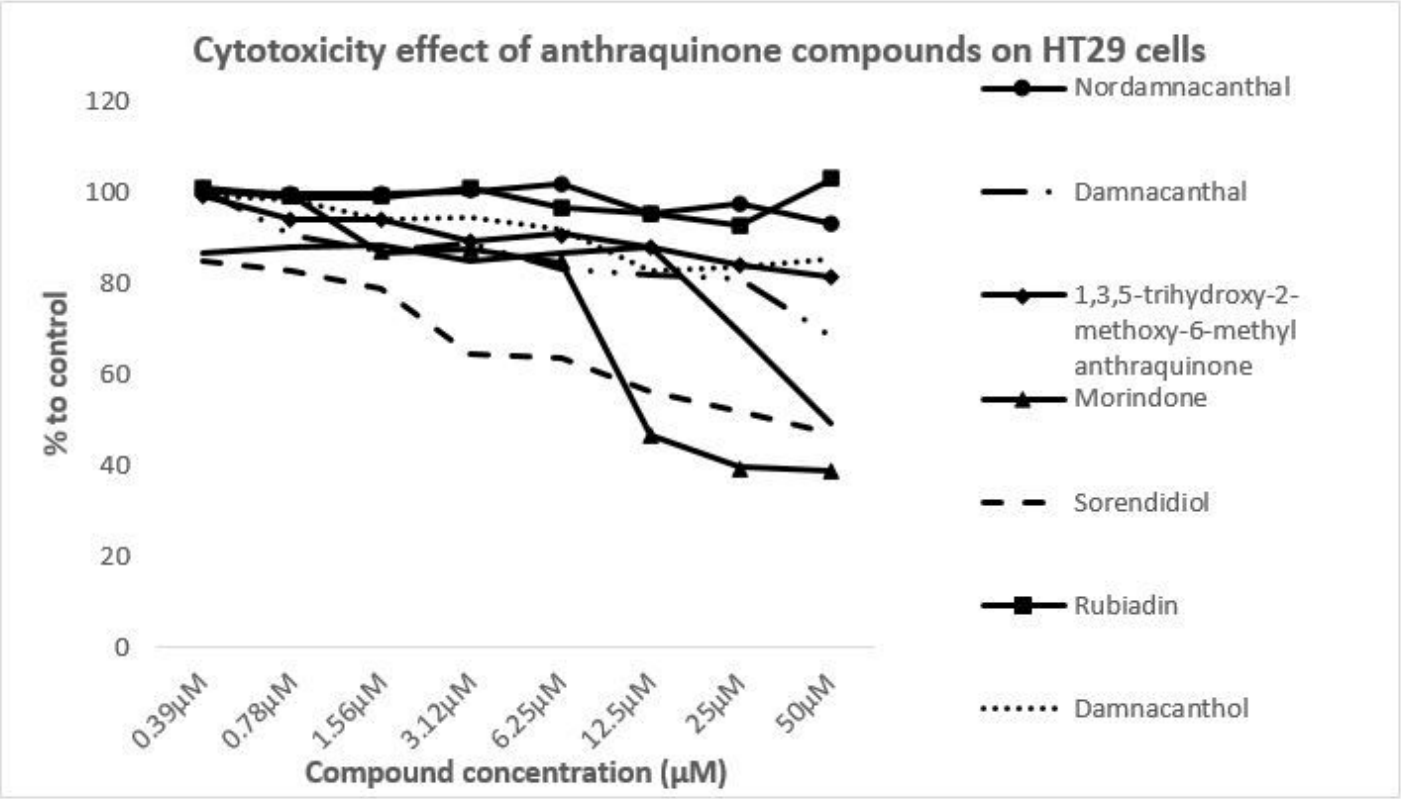

Figure 5

Cytotoxicity effect of anthraquinone compounds 1-8 on HT29 cells after 72 hours treatment.

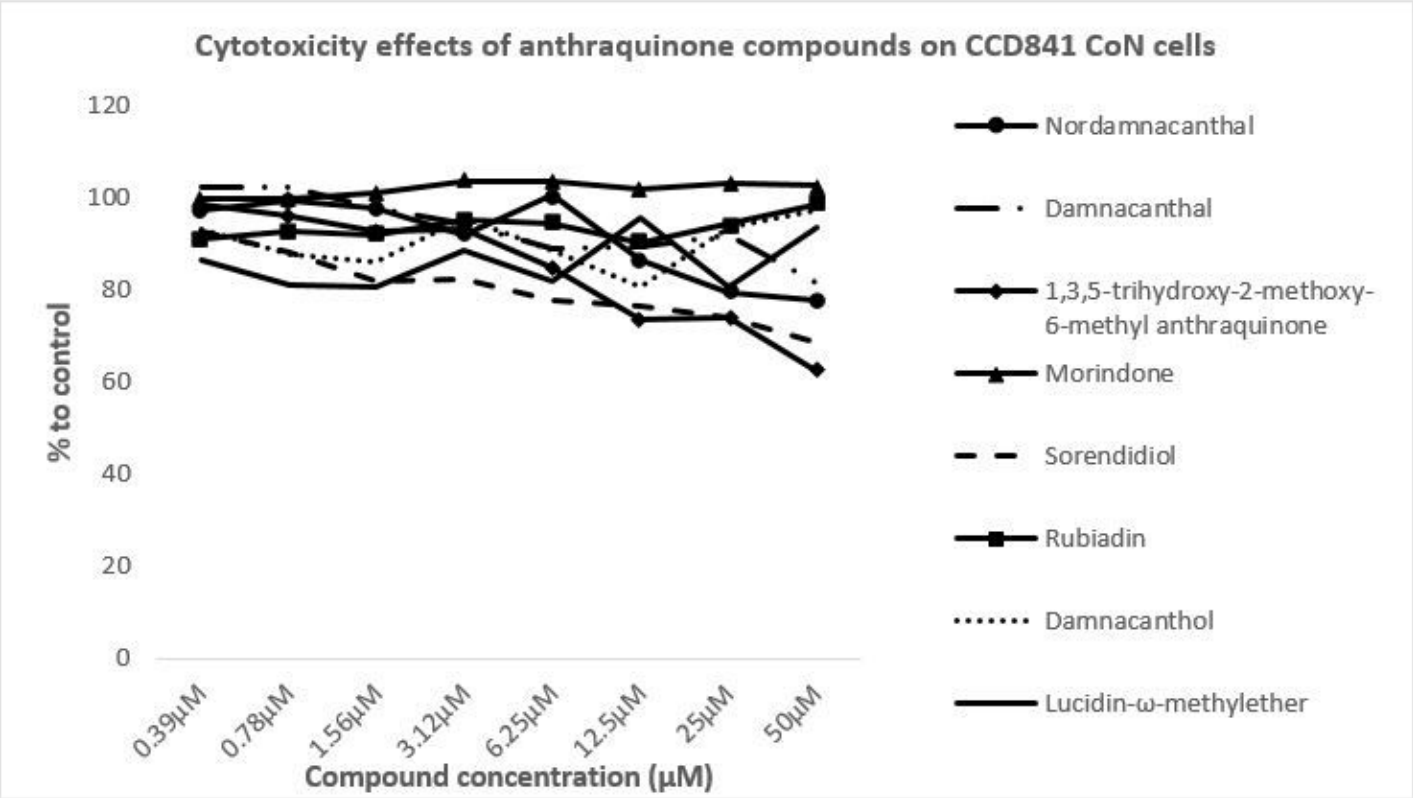

Figure 6

Cytotoxicity effect of anthraquinone compounds 1-8 on CCD841 CoN cells after 72 hours treatment.

Supplementary Files

This is a list of supplementary files associated with this preprint. Click to download.

- SupplementaryMaterials.docx